International Conference on Space Optics—ICSO 2018

Chania, Greece

9–12 October 2018

Edited by Zoran Sodnik, Nikos Karafolas, and Bruno Cugny

Active correction system of a deployable telescope for Earth observation

Dennis Dolkens

Gijsbert Van Marrewijk

Hans Kuiper

International Conference on Space Optics — ICSO 2018, edited by Zoran Sodnik, Nikos Karafolas, Bruno Cugny, Proc. of SPIE Vol. 11180, 111800A · © 2018 ESA and CNES · CCC code: 0277-786X/18/$18 · doi: 10.1117/12.2535929

Active Correction System of a Deployable Telescope for Earth Observation

Dennis Dolkens*, Gijsbert van Marrewijk, Hans Kuiper
Delft University of Technology, Faculty of Aerospace Engineering
Kluyverweg 1, 2629 HS Delft

ABSTRACT

Deployable optics can bring major cost reductions to the field of Earth Observation. One of the key challenges in the development of a deployable optical system, however, is making sure that it can meet its performance targets following its deployment. In this paper, a novel active correction system for a deployable telescope is described. The correction system co-aligns and phases the primary mirror segments and subsequently corrects remaining aberrations using a deformable mirror. A novel phasing sensor called PistonCam can bring telescope segments into phase while the telescope is staring at extended scenes. By only sampling segment boundaries, PistonCam is able to isolate piston and tip/tilt errors which allows the errors to be corrected more effectively. After phasing process has been completed, a moving scene sharpness optimization technique is used to correct the remaining aberrations with a deformable mirror, The technique does not require a constant scene, unlike existing sharpness optimization techniques. As such, the telescope does not need to track a ground scene during the correction process. The technique can also be used for continuous correction of telescope deformations. The active optics system offers robust aberration correction, is computationally inexpensive and requires limited additional optical hardware.

Keywords: Active Optics, Telescopes, Deployable Telescope, Optical Design, Segmented Telescope

1. INTRODUCTION

Deployable Optics have the potential to revolutionize the Earth Observation (EO) market, by drastically reducing the launch volume and mass of a telescope systems. Currently, the highest resolution EO images commercially available are obtained by Worldview-3 and Worldview-4. These system are heavy and expensive, weighing over 2000 kg and costing hundreds of millions of dollars.

The Deployable Telescope, being developed at Delft University of Technology, aims to provide the same resolutions as current state-of-the-art commercial EO systems at a drastically reduced cost. The telescope has been designed for the specifications given in Table 1, which were based on the specifications of Worldview-3[1].

Table 1. Design specifications of the deployable telescope

Aperture Diameter		1.5 m
Focal Length		11 m
Orbital Altitude		500 km
Swath Width		5 km
Cross-Track Field of View		0.6°
GSD	Panchromatic (450-650 nm)	25 cm
	Blue (450-510 nm)	100 cm
	Green (520-580 nm)	100 cm
	Yellow (580-630 nm)	100 cm
	Red (630 – 700 nm)	100 cm

*d.dolkens@tudelft.nl

The optical design of the telescope is based on an annular field Korsch three mirror anastigmat[2]. The design was optimized to provide a diffraction limited image quality across the entire field of view. During the optimization process, degradations due to deployment tolerances and stability tolerances were taken into account. A freeform tertiary mirror was used to improve the optical performance in the corner, while maintaining a compact design.

The primary mirror of the telescope has been split up in four mirror segments, that can be folded alongside the instrument bus during launch. The aperture segments are tapered in the centre. This creates additional area in the centre of the aperture, leading to improved image contrast. Furthermore, the segments are now adjacent to one another in the central ring of the pupil, which proves to be a valuable feature that can be used by the phasing systems. In Figure 1, the optical design and current mechanical design of the deployable telescope is shown.

An end-to-end model was developed to analyse the interaction between all aspects affecting the performance of the telescope system, ranging from thermo-mechanical deformations to image processing techniques. At the core of the model lies an optical raytracer, called FORTA (Fast Optical RayTrace Application). FORTA is a Matlab based raytrace program that was developed from the ground up for raytracing segmented telescope systems. In [3], more information about the model is provided. Throughout this paper, FORTA has been used for all optical analysis work shown.

One of the key challenges that must be addressed to ensure that the deployable telescope can meet a diffraction limited performance is the alignment and co-phasing of the mirror segments. After deployment, the four segments need to be pointed in the same direction and brought into phase with an accuracy of just 10 nm. Meeting such tight requirements is impossible without a sophisticated active optics system.

In this paper, an overview is presented of the active optics system developed for the Deployable Telescope. The paper will start with a section about the deployment budget which was derived for the telescope, which will serve as starting point of the design of the active optics system. Subsequently, the phasing system of the telescope is described. Finally, the correction of remaining aberrations using a deformable mirror is described.

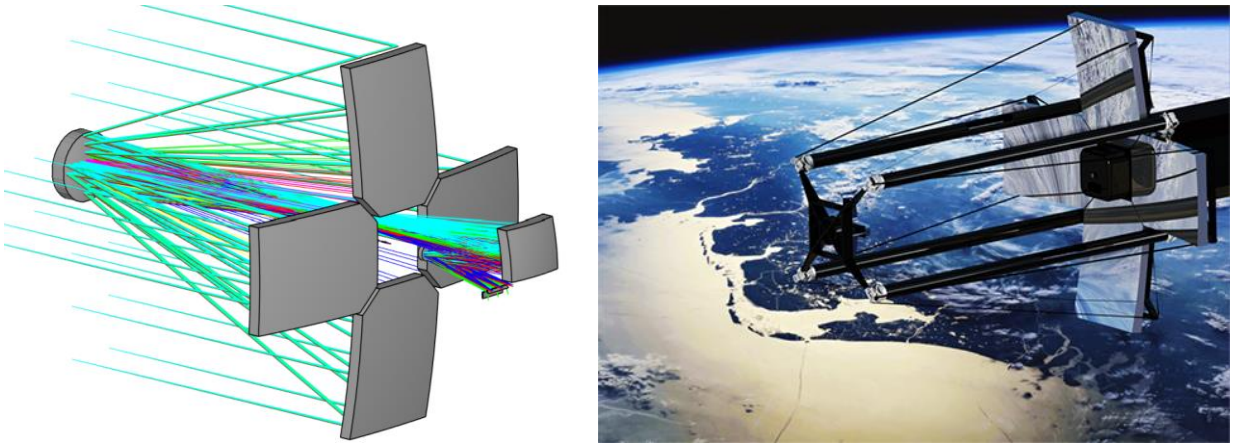

Figure 1. Optical and mechanical design of the Deployable Telescope

2. DEPLOYMENT BUDGET

Due to deployment errors and launch vibrations, the optical elements of the telescope are unlikely to be in their specified position righter after deployment. A deployment budget was derived, which specifies how large the deployment errors can be for the system to still meet its performance targets. The degree to which these errors can be allowed depends on how well the active optics system is able to correct for them. To a large extend, this is limited by the number of degrees of freedom that the telescope can actuate.

The deployable telescope will feature three actuators underneath each mirror segment to control three degrees of freedom to co-align and phase the mirror segments. In addition, a deformable mirror will be positioned in the exit pupil plane to

correct remaining aberration, either resulting from decentre errors of the primary mirror segments or from misalignment of the secondary and tertiary mirrors. It is currently not planned to include actuators on the secondary mirror. Doing so would increase the mass at the tip of the deployable boom, thus making the system more sensitive to microvibrations resulting from the ADCS system.

A consequence of this choice is that tight deployment tolerances on the secondary and tertiary mirrors must be met to ensure that the performance in the edges of the field of view remains acceptable. The secondary mirror is not located in a pupil plane and as such, aberrations introduced by misalignment of this mirror can only be corrected for one field at a time. For other fields, residual field-dependent aberrations will result in a loss of performance.

In table 2, the deployment budget of the deployable telescope is given. The values give the maximum allowable offsets compared to the nominal design for which the active optics system would be able to achieve a diffraction limited image quality across the complete field of view. The budget was tested in an extensive Monte Carlo tolerance analysis.

The most stringent tolerances are placed on the primary mirror segments. Bringing the segments into phase is critical for reaching a diffraction limited image quality. A preliminary analysis into actuator systems that can be used for phasing showed that it is hard to design actuators that have a control resolution in the order of 10 nm as well as a large stroke. Therefore, a tight tolerance budget was specified for the mirror segments.

The budget for the tertiary mirror was also tightened to ensure that it has a negligible impact on the performance. Reaching such tolerances is substantially easier for this mirror, since the mirror is not deployable and is enclosed in the housing of the instrument, where the thermal environment is more stable. Tightening the budget on this mirror meant that the budget of the secondary mirror could be loosened, keeping the design of the deployable boom more manageable.

Table 2: Deployment Budget

Element	Position [µm]			Tilt [µrad]			Radius [%]	RMS Shape Error [nm]
	X	Y	Z	X	Y	Z		
M1	2	2	2	2	4	50	$1*10^{-3}$	50
M2	15	15	10	100	100	100	$1*10^{-2}$	25
M3	4	4	4	10	10	50	$1*10^{-3}$	10

3. SEGMENT PHASING AND CO-ALIGNMENT

The first stage in the active correction of the deployment errors is the co-phasing and co-alignment of the mirror segments. In this section, a short overview is provided of available methods for telescope phasing and the design of PistonCam, a novel phasing sensor is described.

3.1 Overview of Existing Technologies

To sense phasing errors, several techniques have been used in ground based astronomical telescopes. In this subsection, a brief overview of these techniques is given.

At first glance, the pyramid wavefront sensor appears as an interesting option to bring the telescope into phase. The sensor can handle discontinuities in the wavefront and therefore sense the piston error of each segment. The method, however, only works with point sources. Since the telescope is designed for Earth Observation, point sources are not available for calibration, unless the telescope is pointed towards a star.

While the traditional Shack-Hartmann sensor and the Extended Scene Shack-Hartmann sensors are insensitive to piston errors, variations of this sensor have been used in the Keck Telescope. The lenslets of this Shack Hartmann sensor are positioned such that the segment boundaries are sampled. By measuring the coherence length (for the broadband phasing algorithm [4]) or through analysis of the Point Spread Function (in the narrow band phasing algorithm [5]), the relative

piston error between two segments can be estimated. The two methods, however, only works for point sources and not for extended scenes.

The usage of phase diversity was also considered to sense phasing errors. Within the scope of the Deployable Telescope project, this technique was primarily considered to retrieve the phase once the images have been send back to the ground. The he phase information would then be used to restore the image. Usage of phase diversity algorithms on board the spacecraft is challenging however, since the algorithms are computationally intensive. Furthermore, it was observed that the reliability of the algorithm started to suffer when phasing errors become larger than several wavelengths. Particularly in the presence of noise, local minima encountered in the optimization may be incorrectly identified as the true value, which, in the worst case, can lead to segments being send in the wrong direction.

A wavefront-sensorless approach was also considered for the phasing the telescope segments, similar to the method described by Paykin et al [6]. In this method, the position of the mirror segments is optimized such that the sharpness observed at the image plane is optimized. The sharpness of the image can be expressed through a sharpness criterion. Several definitions of the criterion are available; the most common one is given in Eq. (1).

$$S = \int dx\, dy\, I^2(x, y) \tag{1}$$

It can be proven that Eq. (1) reaches a maximum when no wavefront aberrations are present in the system [7]. Several optimization techniques can be used to find the optimal position of the mirror segments. One issue that arises when trying to optimize the position of the telescope is the fact that for every integer number of wavelengths, a local maxima is encountered. Since the telescope is looking at polychromatic sources, the optical performance at the points where these maxima occur is significantly lower than when the global maxima has been found. To avoid these local maxima, non-deterministic algorithms can be used, such as Simulated Annealing [6].

A downside of such algorithms is that large numbers of iterations is required, typically several thousands. This limits the applicability to the Deployable Telescope. Being in a Low Earth Orbit, the time that is available for staring at a particular ground scene is limited, even if the satellite is tracking it. In addition, it was found that the convergence of the algorithm becomes unreliable when besides piston and tip/tilt errors also higher order aberrations are present.

Summarizing, existing technologies do not provide the phasing capabilities that the Deployable Telescope requires. The techniques used are either incompatible with extended scenes or too slow and unreliable for the aberration types that are encountered.

3.2 PistonCam

To speed up the phasing process, a novel phasing sensor concept was developed, called PistonCam. The optical design is shown in Figure 2. The system will be placed in the intermediate image of the telescope. There are two advantages to choosing this location. First of all, there is ample space available in the intermediate image, compared to the region in vicinity of the primary focal plane. Furthermore, the sensor does not use any light meant for the primary detectors. Since only off-axis light can pass through the field stop, it uses light that would otherwise have been blocked. Secondly, the light reaching PistonCam has not encountered the tertiary mirror and deformable mirror. As such, piston and tip/tilt errors can be better isolated.

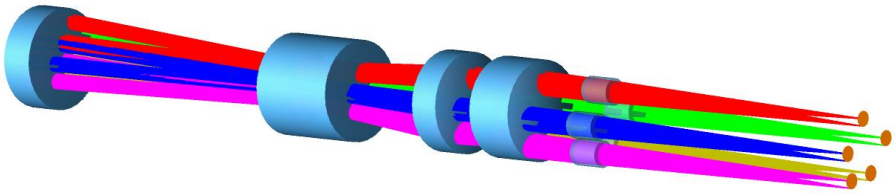

Figure 2. Optical Design of PistonCam

Conceptually, the PistonCam sensor is similar to the Shack-Hartmann-based phasing sensor used on the Keck Telescope. A key difference is that instead of looking at properties of measured point spread functions, the sharpness criterion of each sub-image is optimized. Each sub-image is influenced by only two segments at a time. As a result, the relative piston error between two segments can be found with comparative ease.

The optical design of PistonCam consists of the following components:

- A set of four lenses is used to collimate the light and create a pupil image, as well as correct the wavefront. In the optical design of the telescope, the wavefront quality at the intermediate image was not a design driver, and as such, larger wavefront errors are present here. If the piston errors are to be sensed at the location the intermediate image, these aberrations must first be addressed.
- In the pupil image which has been generated by the lenses, a pupil mask will be placed. This mask ensures that only light from boundary areas in the telescope reaches the telescope. For the current telescope design, four openings, or sub-apertures, will be made in the mask to analyse light from each of the segment boundaries. In addition, a fifth sub-aperture is added that is not affected by any segment edge. Light coming through this aperture can serve as a reference. The size of the sub-apertures in the pupil mask can be tuned. Small apertures have the advantage that the wavefront observed in each channel is dominated by piston and tip/tilt errors, but more noise will be present. For larger apertures, better Signal to Noise Ratios (SNR) can be achieved in each channel, but additional aberrations may cloud the results.
- Behind each sub-aperture of the pupil mask, small lenslets are placed to focus the light onto the detector, creating five small images of the ground scene.

To bring the segments into phase, several steps must be taken. The first step is the co-alignment of the segments, which ensures that all segments are pointed into the same direction. Phasing is only possible after co-alignment; the light coming from two adjacent segments must interfere in the image plane to notice changes in sharpness when the vertical location of a segment is varied. Several optimization methods can be implemented to co-allign the segments. Currently, a Nelder-Mead Simplex method is used, optimizing the sharpness of each channel sequentially. In Figure 3, the optimization process has been visualized for one of the channels.

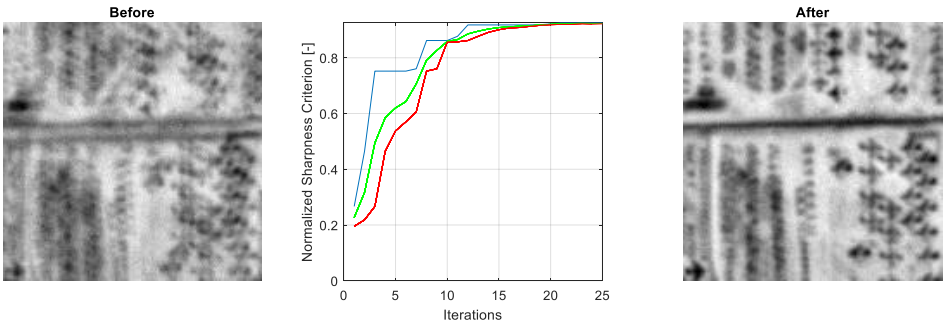

Figure 3. Co-alligment using a Nelder Mead Simplex method. The three curves represent the sharpness criterion at the best, average and worst simplex vertices.

Once all segments have been co-alligned, two of the segments, at opposite sides of the telescope, are scanned through the adjustment range and the image sharpness is recorded throughout the process. In Figure 4, results of a simulation for a system with substantial piston errors is shown. The data has been normalized with respect to the sharpness criterion observed in the reference channel. Since this channel is not free of aberrations either, the normalized criterion can exceed 1.

Based on the data in Figure 4, an estimate of the wavefront at each of the PistonCam channels is obtained. This wavefront estimate is incomplete, however. The sharpness criterion, after all, is not sensitive to a global piston and tilt in the wavefront. The former does not have any effect on the image, while the second only result in a lateral shift of the image. Thus, to compute the desired motion of each of the segments, it needs to be taken into account that the estimated

wavefronts for each of the channels may contain a global piston and tilt component. A linearized model approximating the effect of actuator displacements on the wavefront can be used to calculate the new position of the mirror segments.

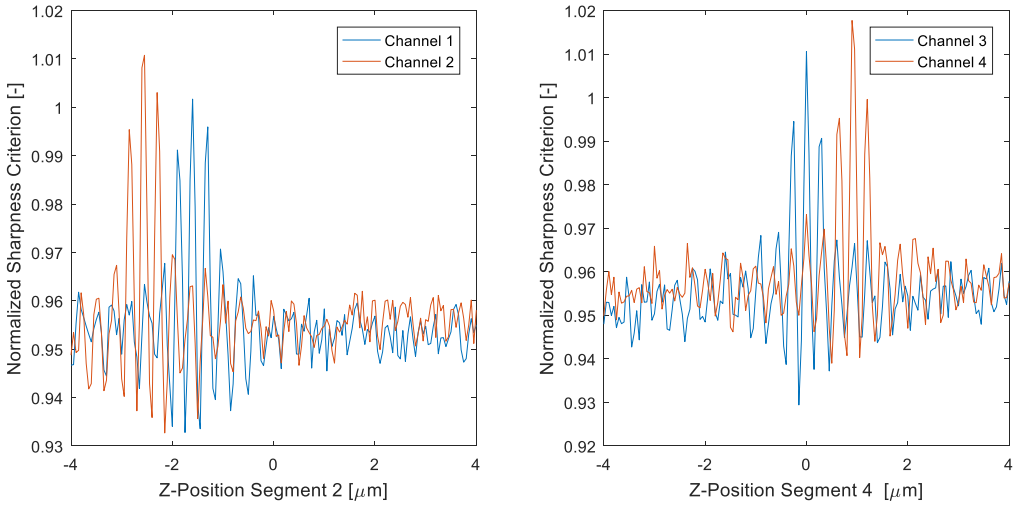

Figure 4. Sharpness variation for z-position of segments

After moving the mirror segments to their calculated position, the sharpness in each channel is measured and compared to the sharpness of the reference channel. If one or more of the channels shows a significantly lower sharpness value than the reference channel, the process is restarted. This typically only when the relative piston error between any two adjacent segments exceeds 4 micron.

Throughout the phasing process, the telescope must track a fixed point on Earth. The sharpness criterion depends to a large extend on the scene. Normalization of the sharpness criterion using the data obtained with the reference channel does not fully remove this scene dependence. The scene that is used for the phasing process can, however, be switched at several instances; each co-alignment step can be performed with a different ground scene.

Extensive Monte Carlo analyses were performed to check the robustness of the phasing algorithm and to see how many iterations are required. In this analysis 1000 optical systems were generated suffering from the deployment tolerances given in Table 2. Only the 100 systems with the worst Root Mean Squared (RMS) Optical Path Difference (OPD) were analysed, since the simulations are computationally intensive. In more than 95% of these cases, the system could successfully bring the segments into phases. The cases which were unsuccessful suffered from intersegment piston errors larger than 5 micron. Running the systems again with an extended scan range, let to successful convergence for these cases as well.

It was found that generally between 400 and 700 mirror positions had to be evaluated before the segments were brought into phase, depending on the severity of the deployment errors. The total duration of the procedure depends on the actuation frequency that can be achieved. To a large extend, this is driven by the stability of the segment support assembly. The time taken for the image read-out and calculation of the sharpness criterion is in the order of milliseconds and as such is not driving the length of the procedure. The design of the mirror support and actuation system not yet complete, but conservative estimates suggest that an actuation frequency of 10 Hz should be achievable, leading to an average phasing duration between 40 and 70 seconds.

After completion of the phasing procedure, the image quality of the telescope is by no means fully corrected. The phasing procedure merely ensures that discontinuities at the segment boundaries are removed. In Figure 5, typical wavefront maps before and after the PistonCam phasing process are shown. As can be seen, after the phasing process, the P-V wavefront error is reduced from 25 to 2.5 waves, but is still very substantial. However, at this point, the wavefront can be considered to be continuous, allowing the remaining aberrations to be corrected by a deformable mirror in the exit pupil plane. In the next section, the procedure that is followed to achieve this will be described.

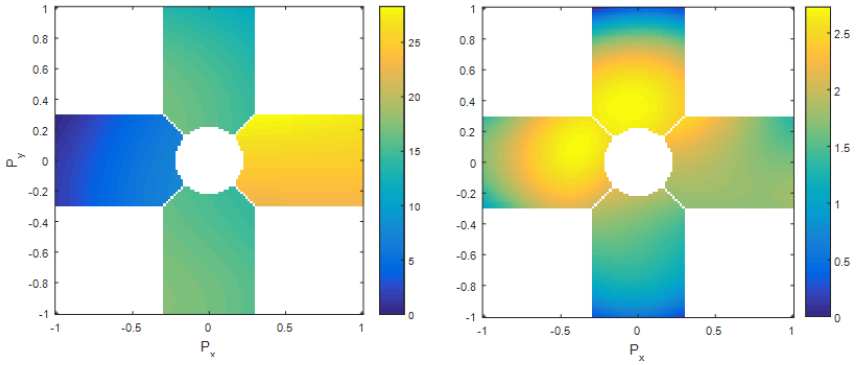

Figure 5. OPD in waves before and after the phasing procedure with PistonCam

4. ABERRATION CORRECTION WITH A DEFORMABLE MIRROR

Once the aperture segments have been phased, the remaining aberrations can be corrected by using a deformable mirror (DM) in the exit pupil plane. In this section, the DM selection and modelling is discussed. After that, the control method of the deformable mirror is described.

4.1 Modelling of the Deformable Mirror

In the search for a suitable deformable mirror for the Deployable Telescope, several types have been considered. The choice was narrowed down to a Monomorph Deformable Mirror (MDM) and a Piezo-Electric Deformable Mirror (PDM). In MDM, actuators act parallel to the mirror surface, causing local bending. In the PDM, push-pull actuators are placed underneath a continuous face sheet to deform the mirror shape. Both deformable mirrors are suitable for use in the telescope, since they can correct the required aberration orders (up to the 7th Zernike order) and, unlike some deformable mirror types, do not require a large ring surrounding the deformable mirror. As such, the mirrors are easier to integrate in the system.

To model the performance of each deformable mirror types, specific surface types were added to FORTA. For the MDM mirror, measured influence functions of the CILAS MONO85-60 DM [8] were used to create a realistic mirror model. The response of each actuator was decomposed into a large number of Zernike terms.

For the PDM mirror, a model was developed using analytical plate deformation equations[9]. In FORTA, the actuator inputs are commanded as zero-load deflections of the actuators. With a model for the actuator and plate stiffness, the resulting deformation can be calculated analytically anywhere on the face sheet. The model was verified using data provided by TNO relating to their DM currently under development for use in space instrumentation[10].

The deformable mirrors can be used to model various operating modes in which a deformable mirror can be used. With modal control, first of all, the DM corrects a certain combination of aberration modes, for instance represented by Zernike functions. When zonal control is used, on the other hand, the shape of the deformable mirror is controlled by steering individual actuators. Besides the capability of modelling different operating modes, the models are more capable for evaluating the effect of high frequency residual errors than when the deformable mirror is simply represented by a set of basis functions.

4.2 Wavefront Optimization Algorithms

To correct the wavefront of the telescope using extended scenes as a source, three approaches can be used. An extended scene Shack-Hartman can be used to directly measure the wavefront, phase diversity can be used to retrieve the phase from two images differing by a known phase error, or the image sharpness can be iteratively optimized. Each of the methods has been analysed within the scope of the Deployable Telescope Project. In this paper, emphasis will be placed on sharpness optimization, since the method appears to be the most promising for the system. The method requires little

additional optical hardware, unlike the Shack Hartmann sensor, and is computationally inexpensive, unlike phase diversity. Furthermore, the method is sensitive to piston errors. If any minor phasing errors were to remain after the phasing process, these errors can, at least partially, be corrected by the deformable mirror.

When sharpness correction is applied such as described in existing literature [6, 7, 11], a major downside of the approach is that typically a static scene is required throughout the optimization process. For a telescope in a Low Earth Orbit, ground scene tracking must therefore be used. Since the optimization is to be performed for a large number of variables, in the case of the Deployable Telescope more than 30, a large number of iterations is required to reach an optimal performance. During the optimization process, regular push-broom operation of the instrument cannot proceed and for large aberrations, the calibration may need to be restarted a number of times after the line of sight between the scene and the telescope has changed too much.

To address these limitations, a new method was developed called Dynamic Scene Image Optimization (DSIO). The method is based on a Parallel Stochastic Gradient optimization method and has been visualized in Fig 6. The method requires two linescan detectors, one placed just behind the other in the along track direction. As the satellite flies over the Earth, the first detector is used to capture an image of the ground. The sharpness of the scene is evaluated, and a random perturbation is given to the deformable mirror. Around 10 milliseconds later, the same scene enters the field of view of the second detector and the sharpness is again evaluated. The two measurement of the sharpness are used to approximate the gradient. Using this gradient, a new control signal is calculated and applied to the deformable mirror. The process is repeated until the maximum number of iterations has been reached. Throughout the optimization, the variance of the step size is gradually reduced to ensure that the optimization converges to a stable value towards the final iteration.

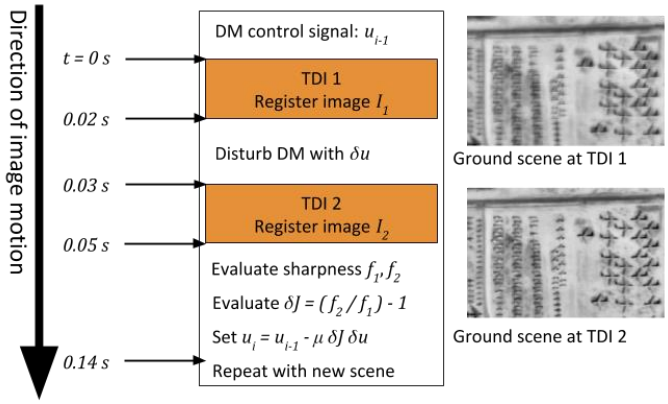

Figure 6. Optimization Process for an extended scene using the Dynamic Scene Image Optimisation Method

The sharpness optimization is performed in two steps. A course calibration is performed first. During this process, the deformable mirror is steered using modal control. The goal of this calibration step is to address large low order aberrations that may be present in the image. Subsequently, a fine calibration step is performed, during which higher order aberrations are addressed with zonal control.

In Figure 7, the results of a simulation of the DSIO method is shown. The simulation was performed with a PDM deformable mirror, using an image set retrieved from Google Earth for a ground track through North America. The Strehl Ratio and RMS OPD have been charted throughout the optimization process. Coarse calibration brings the Strehl ratio on the central field of detector 1 to 0.80, while fine calibration increases this to 0.92 before levelling out around iteration 800. The RMS OPD is reduced from 0.7λ to 0.05λ.

Figure 8 shows the exit pupil OPD before calibration, after coarse calibration and after fine calibration of the DM. It shows that the peak-to-valley OPD is reduced from more than 3λ to less than 0.6λ after coarse calibration, and less than 0.5λ after fine calibration. Although the peak-to-valley wavefront error is still quite large, it has limited effect on the image quality, mainly because extremes in the wavefront map are largely confined to small areas of the pupil, close to segment edges.

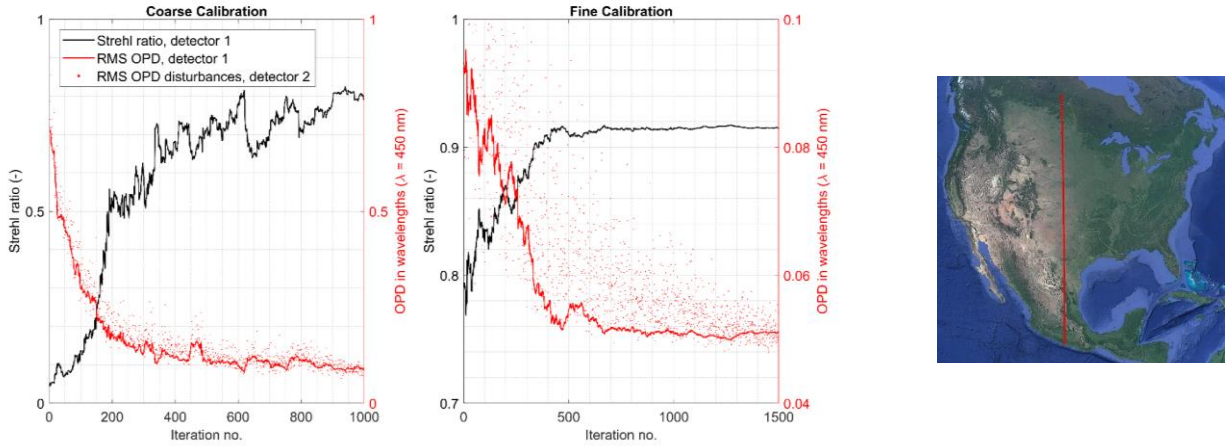

Figure 7. Simulated Strehl ratio and OPD with PDM calibration via the stochastic gradient descent algorithm. Coarse calibration with modal control (left) and fine calibration with zonal control (right). Dots indicate the OPD values on detector 2 when the mirror is disturbed to determine stochastic gradients.

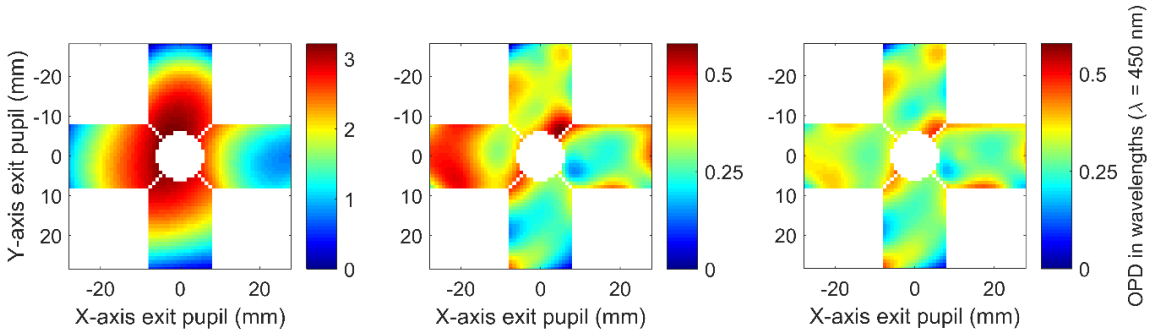

Figure 8. Exit pupil optical path difference for the case shown in Figure after primary mirror segment phasing (left), after PDM modal control (middle) and after PDM zonal control (right).

Although DSIO was primarily developed for periodic aberration correction, it was found that the technique can also be used continuously, to correct aberrations that are arising while the instrument structure is deforming. Using the calibration technique continuously would ensure that the telescope can maintain its calibrated state for a much longer amount of time.

5. CONCLUSIONS AND FUTURE WORK

In this paper, an innovative active optics system for a Deployable Telescope was described. The system can be used to correct deployment errors of the telescope by actuating the position of each of the mirror segments in three degrees of freedom and subsequent optimization of the shape of a deformable mirror.

A novel phasing sensor named PistonCam has been developed to co-align and phase the primary mirror segments. The system can bring telescope segments into phase while the telescope is staring at extended scenes. By only sampling segment boundaries, PistonCam is able to isolate piston and tip/tilt errors which allows the errors to be corrected more effectively.

After the phasing process has been completed, a moving scene sharpness optimization technique is used to correct the remaining aberrations. The technique does not require a constant scene, unlike existing sharpness optimization techniques. As such, the telescope does not need to track a ground scene during the correction process. The technique can also be used for continuous correction of telescope deformations.

Although the techniques described in this paper were optimized for the deployable telescope concept described in the introduction, the techniques can easily be adapted to suit other projects. By changing the pupil mask of PistonCam and re-arranging the lenslets, the system can be adapted to suit almost any pupil shape. The system may be particularly suitable for use on future geostationary segmented telescope systems. Moving scene sharpness optimization, on the other hand, can be directly applied in any push-broom EO system, by adding an additional line scan detector next to the primary one.

Within the scope of the work presented in this paper, future work consists primarily of the refinement of the algorithms to improve their speed and robustness. Furthermore, work will be done towards the experimental validation of the calibration techniques.

ACKNOWLEDGEMENTS

The authors would like to thank ESA and TNO for funding this research through the NPI-program. Furthermore, we would like to thank TNO and CILAS for providing valuable data about their deformable mirrors, which has helped us build much more sophisticated DM models for simulations.

REFERENCES

[1] Digital Globe. *Worldview 3, Above+Beyond*. 2014, 22-11-2014]; Available from: http://worldview3.digitalglobe.com/.
[2] Korsch, D., *Anastigmatic three-mirror telescope.* Appl. Opt., 1977. **16**(8): p. 2074-2077.
[3] Dolkens, D. and H. Kuiper. *Design and end-to-end modelling of a deployable telescope*. in *International Conference on Space Optics—ICSO 2016*. 2017. International Society for Optics and Photonics.
[4] Chanan, G., et al., *Phasing the mirror segments of the Keck telescopes: the broadband phasing algorithm.* Applied Optics, 1998. **37**(1): p. 140-155.
[5] Chanan, G., C. Ohara, and M. Troy, *Phasing the mirror segments of the Keck telescopes II: the narrow-band phasing algorithm.* Applied Optics, 2000. **39**(25): p. 4706-4714.
[6] Paykin, I., et al., *Phasing a segmented telescope.* Physical Review E, 2015. **91**(2): p. 023302.
[7] Muller, R.A. and A. Buffington, *Real-time correction of atmospherically degraded telescope images through image sharpening.* JOSA, 1974. **64**(9): p. 1200-1210.
[8] Cousty, R., et al. *Monomorph deformable mirrors: from ground-based facilities to space telescopes*. in *International Conference on Space Optics—ICSO 2016*. 2017. International Society for Optics and Photonics.
[9] Apollonov, V.V., et al., *Analytic model of an adaptive mirror in the form of a thin plate with discrete actuators.* Soviet Journal of Quantum Electronics, 1990. **20**: p. 1414.
[10] Kuiper, S., et al. *Electromagnetic deformable mirror development at TNO*. in *SPIE Astronomical Telescopes+ Instrumentation*. 2016.
[11] Murray, L., *Smart optics: wavefront sensor-less adaptive optics—image correction through sharpness maximisation.* NUI Galway, 2006.